Effects of electron correlations and chemical pressures on superconductivity of β''-type organic compounds

Shusaku Imajo [1,2,*] Hiroki Akutsu,[1] Akane Akutsu-Sato, Alexander L. Morritt,[3] Lee Martin,[3] and Yasuhiro Nakazawa[1]

[1]*Graduate School of Science, Osaka University, Toyonaka, Osaka 560-0043, Japan*
[2]*Institute for Solid State Physics, University of Tokyo, Kashiwa, Chiba 277-8581, Japan*
[3]*School of Science and Technology, Nottingham Trent University, Clifton Lane, Nottingham NG11 8NS, United Kingdom*

We investigate low-temperature electronic states of the series of organic conductors β''-[bis(ethylenedithio)tetrathiafulvalene]$_4$[(H$_3$O)M(C$_2$O$_4$)$_3$]G, where M and G represent trivalent metal ions and guest organic molecules, respectively. Our structural analyses reveal that the replacement of M and G give rise to systematic change in the cell parameters, especially in the b-axis length, which has a positive correlation with the superconducting transition temperature T_c. Analysis of temperature and magnetic field dependences of the electrical resistance including the Shubnikov–de Haas oscillations elucidates that the variation of charge disproportionation, the effective mass, and the number of itinerant carriers can be systematically explained by the change of the b-axis length. The changes of the transfer integrals induced by stretching/compressing the b axis are confirmed by the band calculation. We discuss that electron correlations in quarter-filled electronic bands lead to charge disproportionation and the possibility of a novel pairing mechanism of superconductivity mediated by charge degrees of freedom.

Superconductivity dominated by electron correlations often appears in nearly-half-filled electronic bands, where an antiferromagnetic Mott insulating state is easily formed by on-site Coulomb repulsion U. In such cases, the superductive regions are located in close proximity to the magnetic Mott phases in electronic phase diagrams [1–3]. Therefore, unconventional pairing related to magnetic spin fluctuations has been suggested to provide an understanding of the mechanisms of the superconductivity. Indeed, the highest critical temperatures T_c are normally observed on the verge of the magnetic phases because the quantum fluctuation coming from the spin degree of freedom is strongly enhanced. High-T_c cuprates [1], heavy fermion superconductors [2], and dimer-Mott-type organic superconductors [3] have been discussed as such candidates of spin-fluctuation-mediated superconductors. Other degrees of freedom, such as orbital (multipole) [4,5] and charge [6], have also been proposed as origins of the pairing in some superconductors, e.g., iron-based compounds and cage compounds. However, it is difficult to examine the relationship between the quantum degrees of freedom and superconductivity because the number of such exotic superconductors is rather small and the pairing states are often in complicated situations due to the coexistence/competition of some degrees of freedom.

---

*imajo@issp.u-tokyo.ac.jp

Recently, β''-type organic charge-transfer salts consisting of bis(ethylenedithio)tetrathiafulvalene (BEDT-TTF) molecules with counteranions and guest solvent molecules have drawn extensive attention because they are expected to have a novel Cooper pairing mechanism related to the charge degrees of freedom [6–15]. The critical temperatures T_c of some β''-type salts are relatively high around 7–8 K, which is almost comparable to the T_c of well-known higher-T_c dimer-Mott organic superconductors κ-(BEDT-TTF)$_2X$. Also, the strong-coupling superconductivity with the large superconducting energy gap $\Delta \sim 2.5k_BT_c$ is expected for β''-(BEDT-TTF)$_4$[(H$_3$O)Ga(C$_2$O$_4$)$_3$]PhNO$_2$ [16,17]. As is shown in Fig. 1(a), the universal phase diagram of the β''-type salts proposed in earlier works [11–15] contends that the superconducting phase is adjacent to the charge-ordered (CO) phase caused by intersite Coulomb repulsion V. It implies that the CO phase appears as an underlying phase for the emerging superconductive phase. Figure 1(b) displays a crystal structure of one such example, a series of the β''-type salts β''-(BEDT-TTF)$_4$[(H$_3$O)M(C$_2$O$_4$)$_3$]G (abbreviated as M/G in this paper), composed of BEDT-TTF, tris(oxalato)metallate ions M(C$_2$O$_4$)$_3{}^{3-}$, and guest molecules G. The β''-type salts are classified as non-dimeric-type organic compounds due to the absence of dimerization of the BEDT-TTF molecules. As the nondimeric feature and the valence (BEDT-TTF)$^{0.5+}$ make the energy band quarter filled, magnetic degrees of freedom are expected to be quenched in uniform CO states. Some earlier works [18–20] suggest that the T_c of the series also exhibits chemical pressure effect associated with the universal phase diagram, depending on the volume [19,20] and length of the guest molecules [18] of the salts. In this work, to elucidate the electronic states of the β''-type salts in more detail, we investigate the low-temperature electronic properties by means
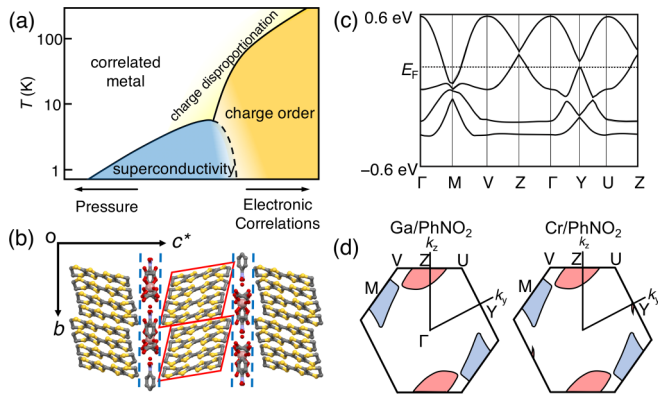
FIG. 1. (a) Schematic phase diagram of quarter-filling β''-type organic conductors showing that the superconducting phase is located in proximity to the charge-ordered phase. (b) Interlayer packing structure of the present salts β''-(BEDT-TTF)$_4$[(H$_3$O)M(C$_2$O$_4$)$_3$]G. The red rhombi indicate tetramers of the BEDT-TTF molecules. The blue dashed lines denote the region of the insulating layer composed of [(H$_3$O)M(C$_2$O$_4$)$_3$]$^{2-}$ and G. (c) Band structure of one of the salts β''-(BEDT-TTF)$_4$[(H$_3$O)Cr(C$_2$O$_4$)$_3$]PhNO$_2$. (d) Fermi surface and first Brillouin zone of β''-(BEDT-TTF)$_4$[(H$_3$O)Ga(C$_2$O$_4$)$_3$]PhNO$_2$ and β''-(BEDT-TTF)$_4$[(H$_3$O)Cr(C$_2$O$_4$)$_3$]PhNO$_2$ derived from the band calculation.

of electrical transport measurements with systematic changes of the electronic states through the chemical substitutions. From the systematic analyses of Shubnikov–de Haas (SdH) oscillations, crystal axes, and band calculations, we clarify the effect of chemical substitution on the electronic state and the relationship between the superconductivity (SC) and physical parameters.

Single crystals of the compounds displayed in Table I are synthesized by electrochemical oxidation methods. The crystal structures and axes of the salts are determined by x-ray diffraction at 298 K. The out-of-plane resistance is measured by a standard four-terminal AC method with current along the c^* axis. Since the crystals harvested from the same batch do not have large sample dependences, each data point in the figures of this paper is obtained by the crystals from one batch for one composition. Four gold wires are attached by carbon paint on both plane surfaces of single crystals. The transport measurements are performed in a ^{3}He refrigerator

TABLE I. Metal ion M and guest molecule G of the salts β''-(BEDT-TTF)$_4$[(H$_3$O)M(C$_2$O$_4$)$_3$]G measured in the present study and their critical temperature T_c.

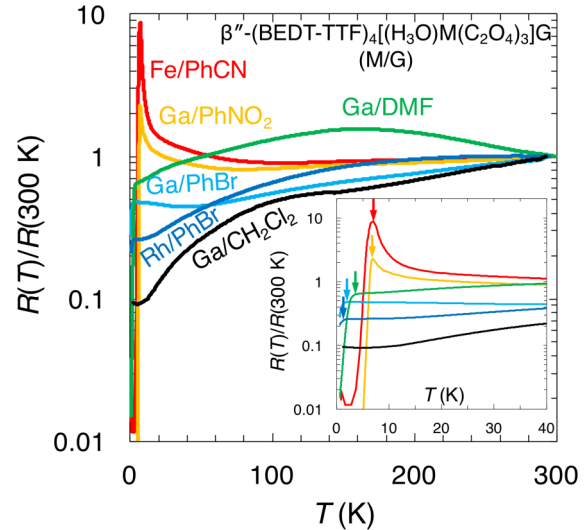| M	G	T_c (K)	M	G	T_c (K)
Fe	C$_6$H$_5$CN	7.2	Ga	2-C$_5$H$_4$ClN	1.7
Ga	C$_6$H$_5$NO$_2$	7.0	Ga	C$_6$H$_5$Cl	no SC
Ga	DMF	4.5	Rh	C$_6$H$_5$Cl	no SC
Ga	C$_6$H$_5$Br	3.0	Ru	C$_6$H$_5$Cl	no SC
Rh	C$_6$H$_5$Br	2.9	Ga	C$_6$H$_5$F	no SC
Ru	C$_6$H$_5$Br	2.8	Rh	C$_6$H$_5$F	no SC
Ga	C$_5$H$_5$N	2.5	Ru	C$_6$H$_5$F	no SC
Ga	C$_6$H$_5$I	2.4	Ga	CH$_2$HCl$_2$	no SC

FIG. 2. Temperature dependences of the scaled electric resistance measured on some salts. The inset shows the expanded graph below 40 K. The arrows indicate the superconducting transition temperatures T_c.

with a 15-T superconducting magnet and a 14-T physical property measurement system (Quantum Design).

As is shown in Fig. 1(b), the series of β''-type salts have a layered structure of alternately stacked BEDT-TTF donor layers, counteranions, and guest solvent molecules layers. The nondimerized arrangement of the donors makes the electronic state quarter filled, since the four BEDT-TTF molecules form charge-transfer salts with the divalent counteranions [(H$_3$O)M(C$_2$O$_4$)$_3$]$^{2-}$. Additionally, the counteranion layer has a neutral solvent molecule G aligned along the b axis with commensurate periodicities. The compounds have weak tetramerization (red rhombi), as shown in Fig. 1(b), and therefore the band structure and Fermi surface are semimetallic, as depicted in Figs. 1(c) and 1(d).

Figure 2 presents the temperature dependence of the interlayer electrical resistance for several β''-type compounds in a semilogarithmic plot. The temperature dependence of the salts including the other salts also measured in this work (see Table I) qualitatively reproduced the results of previous works [16,19–26]. The temperature dependence of the electrical resistance above 100 K is moderate in all salts in the plot. The higher-T_c salts, such as Fe/PhCN and Ga/PhNO$_2$, show weak semiconducting behavior down to 10 K and they show an abrupt increase of the resistance below about 10 K, while the lower-T_c salts and no-SC salts such as Rh/PhBr and Ga/CH$_2$Cl$_2$ show only weak semiconducting behavior at lower temperatures [16,19–26]. This feature is shown in the inset of Fig. 2. Since the gradual increase of the resistance upon cooling is found to have a logarithmic temperature dependence $\sim \log T$, the origin is discussed from the viewpoint of weak localization, which was the quantum interference in disordered electronic systems in Ref. [26]. On the other hand, the insulating behavior below 10 K is observed only in the higher-T_c salts. It is considered that the mobility of itinerant carriers is suppressed by developments of charge disproportionation (CD) [7,8,10]. In the case of Ga/PhNO$_2$, the NMR and electron paramagnetic resonance studies [7,8,10] reveal

that the CD appears very close to T_c with large charge imbalance $\Delta\rho \sim 0.5$. The transition temperature to the CD state T_{CD} is about 8.5 K, which is just above $T_c \sim 7.0$ K. This means that the superconductivity occurs in the CD state whose nature is electrically semiconducting. Also, the CD state has itinerant carriers to form the superconductivity, implying the existence of the Fermi surface even in the CD state. The higher-T_c salts have enough strong electron correlation to make the large CD, which is the precursor of the rigid charge-ordered state, in contrast to the case of the lower-T_c salts and no-SC salts. The enhancement of T_c with increasing electron correlation suggests that the superconductivity may be promoted by the charge instability evolved around the verge of the charge-ordered phase.

In order to discuss the difference in T_c, we now turn to the chemical pressure effect against the electronic system through cation and guest molecule substitution. Since the replacement of the trivalent metal ion M and the solvent molecules G does not modify the band filling, but induces local volume change, the substitution must work as the change of the energy dispersion and bandwidth of the π electrons. It should also be mentioned that introduction of magnetic ions like Fe^{3+} ($S = 5/2$) and Cr^{3+} ($S = 3/2$) does not exert a strong influence on the π electrons. Although the interaction between the insulating and conducting layers known as the π-d interaction [27] plays an important role for the electronic state in some organics, the π-d interaction in the present class is negligible because the metal ion M is located in the depth of the tris(oxalato)metallate molecules. This is indeed confirmed by the absence of a difference of T_c between Fe/G ($S = 5/2$) salts and Ga/G (nonmagnetic) salts with the same G [19,20]. To evaluate the chemical pressure effect, T_c is plotted as a function of the respective lattice constants (the a, b, and c axes and volume) at 298 K in Fig. 3. The data reported in previous literature [19–26,28–30] are also included. The correlation coefficient R for each plot reveals that only the length of the b axis has a strong correlation with T_c, $|R| \sim 0.84$, whereas no obvious correlations $|R| < 0.3$ are observed in the plots against the c axis and volume. The weak negative value $R \sim 0.32$ for the a axis should originate from the Poisson effect in the a-b conducting planes and therefore it is reasonable to consider that the b-axis length has the most dominant effect on T_c. In the counteranion layers, the b axis is the direction toward which the guest molecules orient as represented in Fig. 4(a). This indicates that the length of the guest molecules is exactly the main cause of the substitution effect. As we can find in Table I, the salts with the longer guest molecules in Fig. 4(b) such as PhCN indeed show higher T_c whereas salts with the shorter guest molecules such as CH_2Cl_2 do not superconduct. Namely, the electronic states of the present class can be controlled by the b-axis length through the size of the guest molecules, as expected in Ref. [18]. Hereafter, we use the b-axis length to evaluate the electronic states.

For the discussion of the itinerant carriers, the magnetoresistance of some samples at 1.5 K in perpendicular magnetic fields is shown in Fig. 5(a) in descending order of the b-axis length from top to bottom. The abrupt increase of the resistance below 1 T comes from the suppression of the superconductivity. While we see the presence of the negative magnetoresistance of the higher-T_c salts, only positive magne-
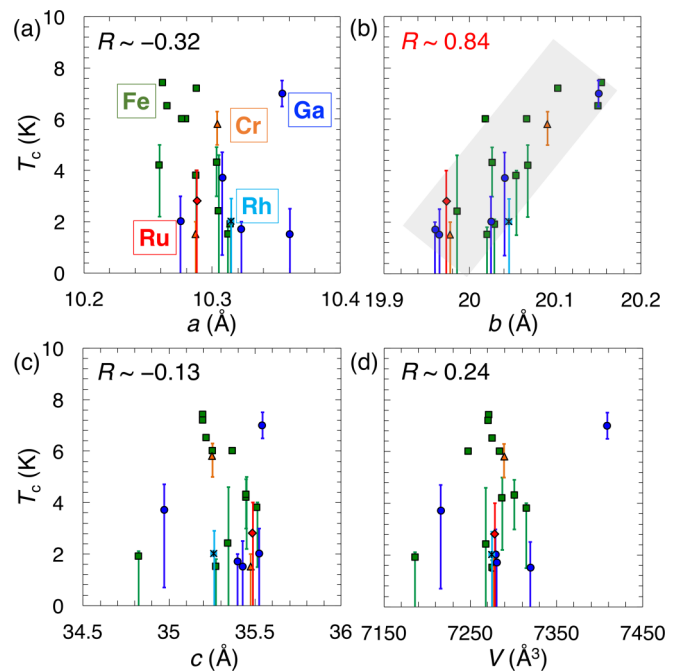

FIG. 3. Superconducting critical temperatures T_c vs lattice constants, (a) a axis, (b) b axis, (c) c axis, and (d) volume, of the β''-type salts and correlation coefficient of the plots R. The plot includes the data reported in previous works [19–26]. The red, blue, green, orange, and cyan symbols represent the center metal ion M of tris(oxalato)metallate as Ru, Ga, Fe, Cr, and Rh, respectively. The T_c of the salts measured in this work is defined by the intersection of the temperature dependence of the resistance of the normal and superconducting states. The bars indicate the onset and zero-resistivity temperatures. The symbols without bars are data taken from previous works for which we cannot determine bars. The error bars of the lattice constants are smaller than the size of the symbols.

toresistance is observed in the lower-T_c and metallic salts. Figure 6(a) shows the normalized slope of the magnetoresistance $(dR/dT)/R$ at 4 T so as to evaluate the change of the magnetoresistance. The magnitude of the negative magnetoresistance is suppressed in compounds with shorter b-axis lengths and it finally converts into a positive magnetoresistance.
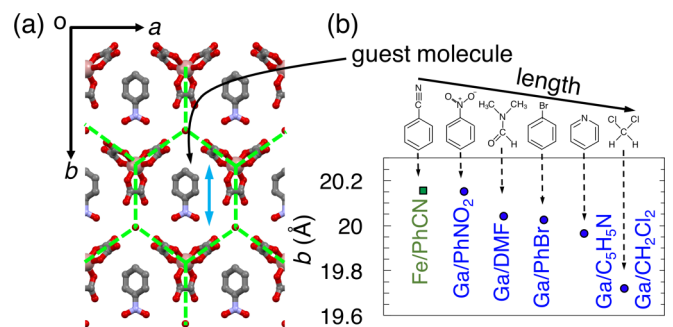

FIG. 4. (a) Arrangement of the guest molecules G in the hexagonal vacancies enclosed by the tris(oxalato)metallate and oxonium ions. (b) Schematic comparison of the length of the guest molecules G and the b-axis length of the β''-type salts containing the respective guest molecules.
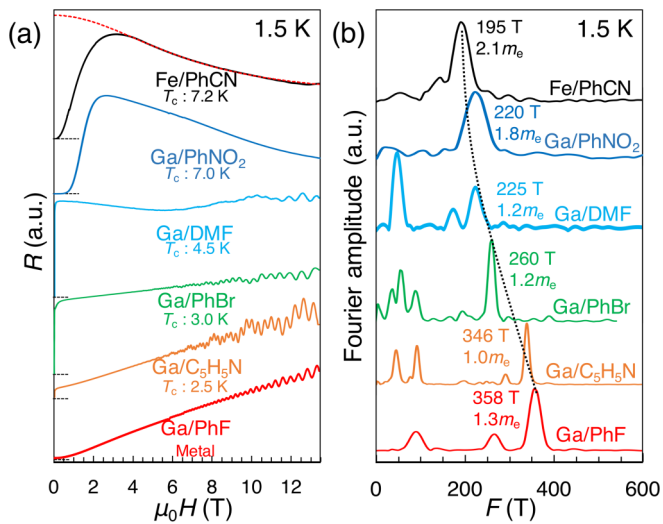
FIG. 5. (a) Magnetoresistance of some β''-type salts at 1.5 K in magnetic fields applied perpendicular to the conducting plane. The data have been offset for clarity. The dashed red line denotes the theoretical calculation expected by the weak localization model [32]. (b) Fourier spectra of the Shubnikov–de Haas oscillations of the samples shown in (a). The values next to the peaks indicate the frequency (upper) and effective mass (lower) of the respective SdH oscillations.

The negative magnetoresistance is discussed in other β''-type salts in terms of Anderson localization with a charge density wave (CDW) [11,31]. References [11,31] suggest that the presence of the CDW can introduce scattering centers, which produce weak localization. Similar to the case of Refs. [11,31], the present result is also explained by the negative magnetoresistance based upon the weak localization proposed by Fukuyama and Yoshida [32], as displayed by the red dashed line of Fe/PhCN in Fig. 5(a), even though the ratio of the charge disproportionation may be rather large as compared with CDWs. The result also agrees with the logarithmic temperature dependence of electrical resistance discussed from the viewpoint of weak localization as mentioned above [26]. The b-axis length dependence of the magnetoresistance suggests that the higher-T_c salts have larger electron correlation to make the CD than the lower-T_c salts have. In other words, the electron correlation of the present class is also related to the b-axis length, similar to T_c.

In the magnetoresistance curves at lower temperatures, SdH oscillations are observed in all salts except for the $M =$ Ru cases. The higher-T_c salts do not have large oscillations as compared with those of lower-T_c ones, but tiny modulation of the resistivity certainly appears in the higher-field region above 10 T. The smaller amplitude of the oscillation of the higher-T_c salts may be caused by the enhanced scattering rate owing to the coexistence with the larger CD. Nonetheless, the observation of the SdH oscillations indicates the existence of the Fermi surface even in the CD state for the higher-T_c salts. Although it is still an open question how the CD state coexists with the conducting part, the electrons in the Fermi surface allow the semiconducting CD state to show the superconductivity. The oscillations of the magnetoresistance can be transformed into the Fourier transform spectrum, which shows peaks at the frequency of the SdH oscillations, as can
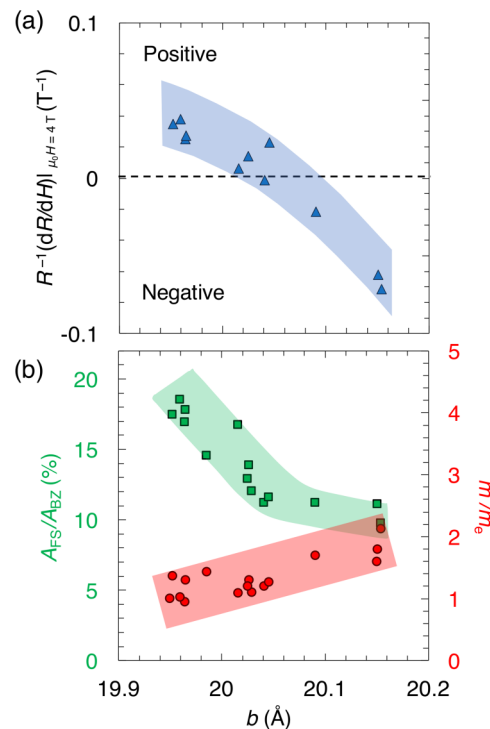

FIG. 6. (a) The b-axis length dependence of the normalized slope of the magnetoresistance $(dR/dT)/R$ at 4 T. The sign of the value corresponds to the sign of the magnetoresistance. (b) Percentage of the cross-sectional area of the electron pocket and the first Brillouin zone (green, the left axis) and the effective mass (red, the right axis) as a function of the b-axis length.

be seen in Fig. 5(b). The higher-T_c salts show only one peak that corresponds to the electron and hole pockets of which the cross-sectional area of the Fermi surface is the same as expected in the simple compensated metal. This is consistent with the results of the previous SdH study by Akutsu and co-workers [16,20] and the calculated Fermi surface reported in Ref. [16]. In contrast to this, the lower-T_c salts have some extra peaks [19,28,29]. In the Brillouin zone of the middle-T_c salt Cr/PhNO$_2$ (with $T_c \sim 5$ K) [20] as introduced in Fig. 1(e), we can find that there is an additional tiny hole pocket around the Y point, whereas the higher-T_c salt Ga/PhNO$_2$ does not show. This means that the topology of the Fermi surface changes by the Lifshitz transition when decreasing the b-axis length. When the bandwidth is stretched by the increase of transfer integral concomitant with the contraction of cell parameters, the additional hole pocket can appear at the Y point and all of the Fermi pockets become larger. Hence, the lower-T_c salts have the larger Fermi pockets with the additional small Fermi pocket. The emergence of the additional Fermi pocket gives some peaks in the spectra due to the split of the hole pockets and the formation of new magnetic breakdown orbits. For simplicity of discussion, we hereafter focus on the electron pocket at the M point because it does not split in the scope of the present chemical substitution. The dotted line in Fig. 5(b) is a guide for the eye to emphasize the peak shift of the electron pocket. In Fig. 6(b) we present the ratio of the cross-sectional area of the electron pocket and Brillouin zone A_{FS}/A_{BZ} and the effective mass of the electron

as m^*/m_e against the b-axis length including the data reported in Refs. [19,20,28,29]. The effective mass m^* is derived from the temperature dependence of the amplitude of each peak by using the Lifshitz-Kosevich formula. Similar to the case of the T_c and the magnetoresistance, these parameters also exhibit the clear correlation with the b-axis length. When decreasing the number of conducting carriers, the area of the Fermi surface in the Brillouin zone becomes smaller. Therefore, the diminution of the ratio A_{FS}/A_{BZ} discussed here demonstrates the gradual decrease of the number of conducting carries while the effective electron mass is enhanced in the higher-T_c salts as shown in Fig. 6(b). The extension of the b-axis length due to the replacement by larger guest molecules reduces the transfer integrals in the molecular stacking. Since the band structure of the present salts is semimetallic, this structural change leads to the shrinkage of the size of the Fermi pockets in semimetallic bands accompanied by the reduction of the bandwidth W. The declining W in the salts with a larger b axis should give the augmentation of the electron correlations because of the increase of the V/W ratios. Namely, the electron mass enhancement appears and the growth of charge disproportionation also occurs in the larger b-axis compounds. Hence, these results agree with the electronic phase diagram presented in Fig. 1(a).

In order to confirm these experimental speculations, we perform the band calculation by the extended-Hückel tight-binding method [33] with a unit cell transformation from the C-centered lattice (x, y, z) to the primitive lattice $(z, 0.5x + 0.5y, x)$ [20]. In the present β'' family, there are eight types of transfer integrals (t_1, t_2, p, q, r, a, b, and c) between the BEDT-TTF molecules as shown in Fig. 7(a). We introduce here the averaged transfer integrals—transverse T [$=(t_1 + t_2)/2$], stacking S [$=(2p + q + r)/4$], and diagonal D [$= (a + b + 2c)/4$]—according to the directions and the number of bonds. In the case of the half-filling Mott systems, the electron correlation is described as U/W, where the on-site Coulomb repulsion U is independent of intersite distance. However, the intersite Coulomb repulsion V of the electron correlation in the present quarter-filling system V/W depends on the intersite distance. Since V is inversely proportional to the distance between molecules and W is in proportion to the transfer integrals, the electron correlation can be evaluated as the dimensionless quantities $V/W \sim e^2/\varepsilon_0 T d_T$, $e^2/\varepsilon_0 S d_S$, and $e^2/\varepsilon_0 D d_D$ by the electric charge e, the electric constant ε_0, the transfer integrals, and the average distance between the molecules along the respective directions d_T, d_S, and d_D. Figure 7(b) displays the b-axis length dependence of the electron correlation along each direction. The diagonal electron correlation $e^2/\varepsilon_0 D d_D$ seems to be independent of the b-axis length whereas the other two $e^2/\varepsilon_0 T d_T$ and $e^2/\varepsilon_0 S d_S$ show a positive correlation with the b-axis length. It is natural because the b axis is the direction nearly perpendicular to the D direction while the others possess the component parallel to the b axis. The positive correlation of the two means that the elongation increases the electron correlation because of the reduction of the overlap of the wave function along the b axis. This confirms that the band calculation perfectly demonstrates the above discussion. Hence, our results totally indicate that the transfer integrals along the b axis play an important role for the electronic state. The CD is considered
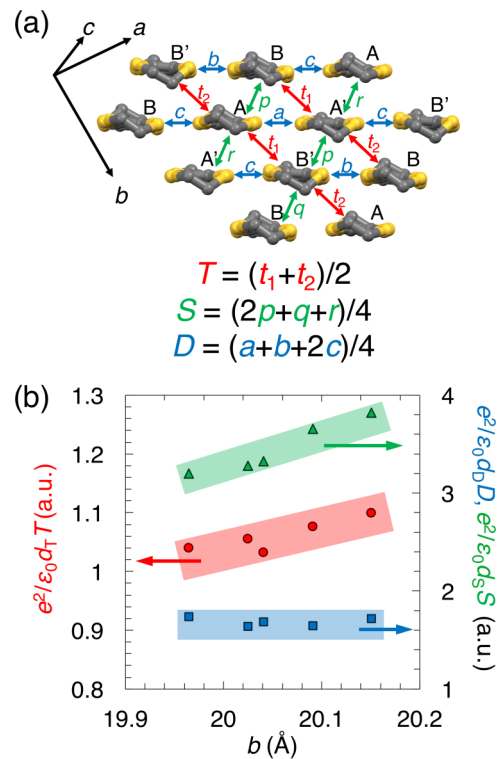

FIG. 7. (a) Placement of the transfer integrals between BEDT-TTF molecules in the conducting layer. The transfer integrals are classified by their directions into three types T, S, and D. The lower formulas represent the definition of the averaged three transfer integrals. (b) The b-axis dependences of the electron correlation along each direction. The evaluation of the electron correlation V/W is described in the text.

as a consequence of the charge instability near the charge-ordered phase by increasing the electron correlation V/W.

Finally, we mention the systematic relation between T_c, the effective mass, and the cross section of the Fermi surface in the case of other quarter-filled β''-type organic superconductors. In Fig. 8 we present the plot of m^* and the SdH frequency F of β''-(BEDT-TTF)$_2$SF$_5$CH$_2$CF$_2$SO$_3$ ($T_c \sim 5.2$ K, $m^* \sim 1.9 m_e$, and $F \sim 200$ T) [34] and β''-(BEDT-TTF)$_2$[(H$_2$O)(NH$_4$)$_2$Cr(C$_2$O$_4$)$_3$]·18-crown-6 ($T_c \sim 4.5$ K, $m^* \sim 1.4 m_e$, and $F \sim 230$ T) [35,36] with the results of the present salts. It is clearly found that the parameters of the two salts fall in the correlation derived from our results. Quite recently, optical measurements [14,15] have pointed out that the superconductivity found in β''-(BEDT-TTF)$_2$SF$_5$CH$_2$CF$_2$SO$_3$ also coexists with a charge order similar to the present case. These facts suggest that the β''-type organics can be universally discussed in a generic phase diagram with the electron correlation like Fig. 1(a) and the superconductivity observed in these β''-type salts should share the same pairing mechanism of the superconductivity. In future work, the symmetry of the superconducting energy gap should be examined for the comprehension of the detailed mechanism of how the superconductivity is formed by the charge fluctuation.

We reported the electrical transport properties of the organic conductors β''-(BEDT-TTF)$_4$[(H$_3$O)M(C$_2$O$_4$)$_3$]G with
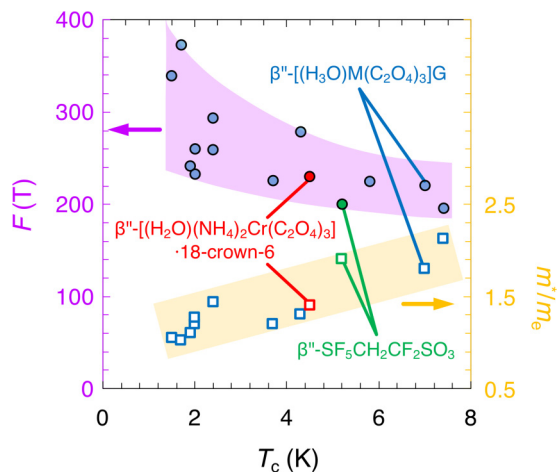
FIG. 8. Comprehensive plot of the frequency of the Shubnikov–de Haas oscillations F (left) and the effective mass m^*/m_e (right) vs T_c for 1/4-filled β''-type organic salts. The colors of the symbols represent the type of counteranions of the β''-type salts as $[(H_3O)M(C_2O_4)_3]G$ (blue), $SF_5CH_2CF_2SO_3$ (green), and $[(H_2O)(NH_4)_2Cr(C_2O_4)_3] \cdot$ 18-crown-6 (red), respectively. The circles denote the data of the frequency and the squares indicate the data of the effective mass.

chemical substitution. From the results of the temperature and magnetic field dependences we found that the semiconducting behavior and negative magnetoresistance observed in the higher-T_c salts originate from the charge disproportionation caused by the stronger electron correlation. We also found that the superconducting transition temperatures are influenced mainly by the b-axis length depending on the length of the guest molecules because the b axis corresponds to the direction of the orientation of the guest molecules in the counterlayer. From the analysis of the Shubnikov–de Haas oscillations it was found that the effective mass and the number of carriers are influenced by the b-axis length. The band calculation also demonstrates the experimental results that the electron correlation reflects the transfer integrals along the b-axis direction. The increase of T_c accompanied by the enhancement of the CD with lengthening the b-axis length suggests that the superconductivity should be mediated by the charge fluctuation evolved at the phase boundary of the charge-ordered phase. Moreover, we found that the present discussion of the electronic state can be applied to the other β''-type salts according to the electron correlation. The superconductivity of the β''-type compounds is universally expected to be produced by the charge fluctuation enhanced near the charge-ordered phase.

[1] C. C. Tsuei and J. R. Kirtley, Rev. Mod. Phys. **72**, 969 (2000).

[2] C. Pfleiderer, Rev. Mod. Phys. **81**, 1551 (2009).

[3] K. Kanoda, J. Phys. Soc. Jpn. **75**, 051007 (2006).

[4] H. Kontani and S. Onari, Phys. Rev. Lett. **104**, 157001 (2010).

[5] M. Tsujimoto, Y. Matsumoto, T. Tomita, A. Sakai, and S. Nakatsuji, Phys. Rev. Lett. **113**, 267001 (2014).

[6] J. Merino and R. H. McKenzie, Phys. Rev. Lett. **87**, 237002 (2001).

[7] Y. Ihara, H. Seki, and A. Kawamoto, J. Phys. Soc. Jpn. **82**, 083701 (2013).

[8] Y. Ihara, M. Jeong, H. Mayaffre, C. Berthier, M. Horvatić, H. Seki, and A. Kawamoto, Phys. Rev. B **90**, 121106(R) (2014).

[9] Y. Ihara, Y. Futami, and A. Kawamoto, J. Phys. Soc. Jpn. **85**, 014601 (2016).

[10] Y. Ihara, K. Moribe, S. Fukuoka, and A. Kawamoto, Phys. Rev. B **100**, 060505(R) (2019).

[11] W. Lubczynski, S. V. Demishev, J. Singleton, J. M. Caulfield, L. du Croo de Jongh, C. J. Kepert, S. J. Blundell, W. Hayes, M. Kurmoo, and P. Day, J. Phys.: Condens. Matter **8**, 6005 (1996).

[12] H. Mori, I. Hirabayashi, S. Tanaka, T. Mori, Y. Maruyama, and H. Inokuchi, Solid State Commun. **80**, 411 (1991).

[13] A. Girlando, M. Masino, J. A. Schlueter, N. Drichko, S. Kaiser, and M. Dressel, Phys. Rev. B **89**, 174503 (2014).

[14] A. Pustogow, Y. Saito, A. Rohwer, J. A. Schlueter, and M. Dressel, Phys. Rev. B **99**, 140509(R) (2019).

[15] A. Pustogow, K. Treptow, A. Rohwer, Y. Saito, M. Sanz Alonso, A. Lohle, J. A. Schlueter, and M. Dressel, Phys. Rev. B **99**, 155144 (2019).

[16] S. Uji, Y. Iida, S. Sugiura, T. Isono, K. Sugii, N. Kikugawa, T. Terashima, S. Yasuzuka, H. Akutsu, Y. Nakazawa, D. Graf, and P. Day, Phys. Rev. B **97**, 144505 (2018).

[17] S. Imajo, Y. Nakazawa, and K. Kindo, J. Phys. Soc. Jpn. **87**, 123704 (2018).

[18] T. G. Prokhorova and E. B. Yagubski, Russ. Chem. Rev. **86**, 164 (2017).

[19] A. I. Coldea, A. F. Bangura, J. Singleton, A. Ardavan, A. Akutsu-Sato, H. Akutsu, S. S. Turner, and P. Day, Phys. Rev. B **69**, 085112 (2004).

[20] A. F. Bangura, A. I. Coldea, J. Singleton, A. Ardavan, A. Akutsu-Sato, H. Akutsu, S. S. Turner, P. Day, T. Yamamoto, and K. Yakushi, Phys. Rev. B **72**, 014543 (2005).

[21] H. Akutsu, A. Akutsu-Sato, S. S. Turner, D. Le Pevelen, P. Day, V. Laukhin, A.-K. Klehe, J. Singleton, D. A. Tocher, M. R. Probert, and J. A. K. Howard, J. Am. Chem. Soc. **124**, 12430 (2002).

[22] L. Martin, A. L. Morritt, J. R. Lopez, Y. Nakazawa, H. Akutsu, S. Imajo, Y. Ihara, B. Zhang, and Y. Guo, Dalton Trans. **46**, 9542 (2017).

[23] T. G. Prokhorova, L. I. Buravov, E. B. Yagubskii, L. V. Zorina, S. S. Khasanov, S. V. Simonov, R. P. Shibaeva, A. V. Korobenko, and V. N. Zverev, CrystEngComm **13**, 537 (2011).

[24] E. Coronado, S. Curreli, C. Giménez-Saiz, and C. J. Gómez-García, Inorg. Chem. **51**, 1111 (2012).

[25] T. G. Prokhorova, L. V. Zorina, S. V. Simonov, V. N. Zverev, E. Canadell, R. P. Shibaeva, and E. B. Yagubskii, CrystEngComm **15**, 7048 (2013).

[26] T. G. Prokhorova, E. B. Yagubskii, L. V. Zorina, S. V. Simonov, V. N. Zverev, R. P. Shibaeva, and L. I. Buravov, Crystals **8**, 92 (2018).

[27] T. Mori and M. Katsuhara, J. Phys. Soc. Jpn. **71**, 826 (2002).

[28] T. G. Prokhorova, L. I. Buravov, E. B. Yagubskii, L. V. Zorina, S. V. Simonov, V. N. Zverev, R. P. Shibaeva, and E. Canadell, Eur. J. Inorg. Chem. **34**, 5611 (2015).

[29] A. Audouard, V. N. Laukhin, L. Brossard, T. G. Prokhorova, E. B. Yagubskii, and E. Canadell, Phys. Rev. B **69**, 144523 (2004).

[30] S. Rashid, S. S. Turner, P. Day, J. A. K. Howard, P. Guionneau, E. J. L. McInnes, F. E. Mabbs, R. J. H. Clark, S. Firth, and T. Biggs, J. Mater. Chem. **11**, 2095 (2001).

[31] P. A. Goddard, S. W. Tozer, J. Singleton, A. Ardavan, A. Abate, and M. Kurmoo, J. Phys.: Condens. Matter **14**, 7345 (2002).

[32] H. Fukuyama and K. Yoshida, J. Phys. Soc. Jpn. **46**, 102 (1979).

[33] T. Mori, A. Kobayashi, Y. Sasaki, H. Kobayashi, G. Saito, and H. Inokuchi, Bull. Chem. Soc. Jpn. **57**, 627 (1984).

[34] D. Beckmann, S. Wanka, J. Wosnitza, J. A. Schlueter, J. M. Williams, P. G. Nixon, R. W. Winter, G. L. Gard, J. Ren, and M.-H. Whangbo, Eur. Phys. J. B **1**, 295 (1998).

[35] L. Martin, J. R. Lopez, H. Akutsu, Y. Nakazawa, and S. Imajo, Inorg. Chem. **56**, 14045 (2017).

[36] A. L. Morritt, J. R. Lopez, T. J. Blundell, E. Canadell, H. Akutsu, Y. Nakazawa, S. Imajo, and L. Martin, Inorg. Chem. **58**, 10656 (2019).